Published in final edited form as:
Clin Cancer Res. 2009 November 1; 15(21): 6639–6648. doi:10.1158/1078-0432.CCR-09-0951.

EGFR Tyrosine Kinase Inhibitor Reverses Mesenchymal to Epithelial Phenotype and Inhibits Metastasis in Inflammatory Breast Cancer

Dongwei Zhang[1,2], **Tiffany A. LaFortune**[1,2], **Savitri Krishnamurthy**[3], **Francisco J. Esteva**[2], **Massimo Cristofanilli**[2], **Ping Liu**[4], **Anthony Lucci**[5], **Balraj Singh**[5], **Mien-Chie Hung**[6], **Gabriel N. Hortobagyi**[2], and **Naoto T. Ueno**[1,2,7]

[1]Breast Cancer Translational Research Laboratory, The University of Texas M. D. Anderson Cancer Center, Houston, TX, USA

[2]Department of Breast Medical Oncology, The University of Texas M. D. Anderson Cancer Center, Houston, TX, USA

[3]Department of Pathology, The University of Texas M. D. Anderson Cancer Center, Houston, TX, USA

[4]Department of Biostatistics, The University of Texas M. D. Anderson Cancer Center, Houston, TX, USA

[5]Department of Surgical Oncology, The University of Texas M. D. Anderson Cancer Center, Houston, TX, USA

[6]Department of Molecular and Cellular Oncology, The University of Texas M. D. Anderson Cancer Center, Houston, TX, USA

[7]Department of Stem Cell Transplantation and Cellular Therapy, The University of Texas M. D. Anderson Cancer Center, Houston, TX, USA

Abstract

Purpose—Inflammatory breast cancer (IBC) is a rare but aggressive type of advanced breast cancer. Epidermal growth factor receptor (EGFR) expression is an independent poor prognostic factor in IBC. The purpose of this study was to determine the impact on IBC tumorigenicity and metastasis of blocking the EGFR pathway.

Experimental Design—IBC cell lines, which express high level of EGFR, were treated with EGFR siRNA and with the EGFR tyrosine kinase inhibitor erlotinib. The role of EGFR in IBC cell proliferation, motility, invasiveness, and change of the expression levels of epithelial-mesenchymal transition (EMT) markers were examined. The role of mitogen-activated protein kinase (ERK) 1/2 in erlotinib activity was also studied. The activity of erlotinib in tumor growth and metastasis was examined in an orthotopic xenograft model of IBC.

Results—Erlotinib inhibited proliferation and anchorage-independent growth of IBC cells, and this inhibition was ERK dependent. Erlotinib inhibited cell motility and invasiveness and reversed the mesenchymal phenotype of IBC cells to epithelial phenotype in three-dimensional culture. Erlotinib dramatically inhibited IBC tumor growth in a xenograft model. Interestingly, erlotinib inhibited

Requests for reprints: Naoto T. Ueno, Department of Breast Medical Oncology, Unit 1354, The University of Texas M. D. Anderson Cancer Center, 1515 Holcombe Blvd., Houston, TX 77030, USA. Phone: 713-792-8754; Fax: 713-794-4385; E-mail: nueno@mdanderson.org.

spontaneous lung metastasis, even at a low dose that had no significant impact on primary tumor growth. These erlotinib-treated tumors were converted to epithelial phenotype from mesenchymal phenotype.

Conclusions—The EGFR pathway is involved in tumor growth and metastasis of IBC. Targeting EGFR through the ERK pathway may represent an effective therapeutic approach to suppress tumorigenicity and prevent metastasis in EGFR-expressing IBC.

Keywords

inflammatory breast cancer; tyrosine kinase inhibitor; EGFR; erlotinib; metastasis

Introduction

Inflammatory breast cancer (IBC) is a rare but very aggressive type of advanced breast cancer that accounts for 1% to 5% of all breast cancer cases in the United States (1,2). IBC can initially present as either stage IIIB locally advanced or stage IV breast cancer (3). IBC is characterized by extensive lymphovascular invasion and is associated with a high risk of distant metastases (4). Even when treated with multimodality strategies including chemotherapy, surgery, and radiation therapy, IBC is associated with a poor long-term outcome and a high risk of recurrence and metastasis compared with non-inflammatory locally advanced breast cancer. The 3-year survival rate among IBC patients is only about 40%, much lower than the 85% 3-year survival rate among patients with non-inflammatory breast cancer (5). To date, effective standard therapies for IBC are limited. Therefore, novel therapeutic approaches need to be developed. Studying the biological basis of IBC will allow us to develop novel targeted therapies to improve the outcome of IBC.

It is reported that up to 30% of IBC patients have distant metastases at the time of diagnosis, in contrast to 5% of patients with non-inflammatory breast cancer (6). The lower survival rate of patients with IBC is thought to be due to the highly metastatic nature of the disease. An important event during malignant tumor progression and metastasis is epithelial-mesenchymal transition (EMT), a process by which cells undergo a morphological switch from a polarized epithelial phenotype to a mesenchymal fibroblastoid phenotype (7–9). EMT is characterized by the loss of epithelial markers (E-cadherin, cytokeratins) and the presence of mesenchymal markers (vimentin, fibronectin). Evidence of the importance of EMT in metastasis includes the fact that reduction of E-cadherin may contribute to metastatic spread of breast cancer (10).

The epidermal growth factor receptor (EGFR/ErbB1) and HER2 (ErbB2), members of the ErbB receptor tyrosine kinase family, are frequently overexpressed in human malignant tumors and are known to drive tumor growth and progression (11–15). Stimulation of EGFR is associated with cell proliferation and with multiple processes involved in tumor progression, invasion, and metastasis (16,17). Overexpression of EGFR is associated with poor prognosis and reduced overall survival in patients with lung cancer (18–20). Therefore, the EGFR signaling pathway has emerged as a promising target for cancer therapy. A number of EGFR tyrosine kinase inhibitors (TKIs) that target EGFR have been developed and used successfully to treat cancer patients. For example, erlotinib, a small-molecule EGFR TKI, is used to treat non-small cell lung cancer, pancreatic cancer, and several other types of cancer (21,22). However, in non-inflammatory breast cancer, EGFR TKIs such as erlotinib and gefitinib have shown minimum clinical activity (23,24). Further, when the activity of an EGFR/HER2 dual tyrosine kinase inhibitor, lapatinib, was tested in IBC, lapatinib exhibited clinical activity only in heavily pretreated HER2-positive IBC (25).

In our previous study, we showed that EGFR overexpression was detected in 30% of IBC patients by immunohistochemical staining. EGFR-expressing IBC was associated with a significantly worse 5-year overall survival rate than EGFR-negative IBC, and EGFR expression was associated with increased risk of IBC recurrence (26). Thus, EGFR may represent a potential therapeutic target in IBC. However, the biological association between EGFR expression and poor prognosis and increased risk of recurrence is not known in IBC, and the impact of EGFR TKIs on metastasis of IBC has not been evaluated.

In the study reported here, we found that erlotinib exhibits ERK-dependent antiproliferative activity in IBC. Furthermore, erlotinib reversed the mesenchymal phenotype of IBC cells to epithelial phenotype in 3-dimensional (3D) culture. More importantly, erlotinib inhibited the tumor growth and spontaneous lung metastasis of IBC in an orthotopic IBC xenograft model. Our study provides a rationale for developing novel treatment strategies targeting the EGFR and ERK pathways to inhibit the growth and metastasis of EGFR-expressing IBC.

Materials and Methods

Cell culture, reagents, and transfection

The human IBC cell line SUM149 (estrogen receptor and progesterone receptor negative; EGFR and HER2 positive) was obtained from the University of Michigan. The SUM149 cells were grown in Ham's F12 medium supplemented with 5% FBS (GIBCO/BRL), 5 μg/ml insulin, and 1 μg/ml hydrocortisone in a humidified atmosphere containing 5% CO_2 at 37°C. The KPL-4 IBC cell line (estrogen receptor and progesterone receptor positive; EGFR and HER2 positive) (27) was kindly provided by Dr. Junichi Kurebayashi (Kawasaki Medical School, Japan) and was maintained in DMEM/F12 medium supplemented with 10% FBS. Erlotinib was purchased from ChemieTek (Indianapolis, IN, USA). The expression vector for HA-tagged constitutively active MEK1 (CA-MEK1) was a gift from P. P. Pandolfi (Harvard Medical School, Boston, MA). Cells were transfected with CA-MEK1 using FuGENE 6 reagent (Roche). Anti-HA antibody was used to detect the expression of CA-MEK1 in IBC cells by western blot analysis following the approach described in our previously published manuscript (28).

Western blot analysis

Western blot analysis was performed as previously described (29). The following antibodies were used (all from Cell Signaling Technology except where indicated): anti-EGFR (Santa Cruz Biotechnology; catalog sc-03), anti-HER2/c-neu (Oncogene Research Products; catalog OP15-100), anti-Phospho-EGFR (Y1173) (Santa Cruz Biotechnology; catalog sc-12351), anti-Akt (catalog 9272), anti-Phospho-Akt (S473) (catalog 9271), anti-ERK 1/2 (catalog 9107), anti-Phospho-ERK 1/2 (T202/Y204) (catalog 9101), anti-HA (Santa Cruz Biotechnology; catalog sc-57592), and anti-β-actin (Sigma-Aldrich; catalog A-5441).

WST-1 assay

A cell suspension of 2,000 cells/90 μl was seeded into each well of a 96-well plate and cultured overnight, after which 10 μl of erlotinib solution at a final concentration ranging from 0.1 to 10 μM was added to the individual wells. The concentrations of erlotinib used in WST-1 assay were chosen based on our previously published manuscript (30). After 3 days of erlotinib treatment, 10 μl of ready-to-use WST-1 (4-[3-(4-iodophenyl)-2-(4-nitrophenyl)-2H-5-tetrazolio]-1,3-benzene disulfonate) reagent (Roche Applied Science) was added directly into the medium, the plates were incubated at 37°C for 1 h, and absorbance was measured on a plate reader at 450 nm. All experiments were done in triplicate. Cell viability was calculated as the percentage of cells killed by the treatment as measured by differences in optical density

between treated and untreated wells. Median inhibitory concentrations were determined from these calculations.

siRNA knockdown

ON-TARGET plus siRNA SMART pools against EGFR, ERK 1/2, and siGENOME Non-Targeting siRNA Pool (control siRNA) were purchased from Dharmacon Research Inc. (Lafayette, CO). RNA interference assay was performed according to the manufacturer's protocol (Dharmacon Research). Briefly, cells were seeded in 6-well culture plates at 30% confluence in culture medium supplemented with FBS. The next day, cells were transfected with siRNA at a final concentration of 100 nM by using Oligofectamine (Invitrogen).

Migration and invasion assay

For trans-well migration assay, SUM149 cells were first treated with erlotinib for 48 h. Then 2.5×10^5 cells were layered in the top chambers of 24-well trans-well plates (BD Biosciences, San Diego, CA; 8-μm pore size) and incubated at 37°C for 6 h in normal culture medium without erlotinib. Cells in the top chamber (nonmigrated) were removed, and cells in the bottom chamber (migrated) were fixed in 20% methanol and stained with 0.1% crystal violet. For quantification, migrated cells were counted from 4 random fields per well from 3 independent experiments. The quantification of cell invasion was performed using Boyden chambers. Cells were treated with erlotinib for 48 h before the assay, and 2.5×10^4 cells were then plated in serum-free medium in the upper chamber of the Boyden chamber coated with Matrigel (BD Biosciences) with serum-containing medium in the lower chamber in the absence of erlotinib. Twenty-four hours later, uninvaded cells were removed from the upper chamber, and the undersides of the membranes were fixed and stained. Invading cells were quantitated by dissolving stained cells in a solution of 4% sodium deoxycholate and colorimetric reading of OD at 595 nm.

Anchorage-independent growth

Soft agar colony-formation assay was performed as previously described (31). Briefly, SUM149 cells (2×10^3 /well) were inoculated into soft agar (0.4%) in culture medium and then plated over a base layer of 0.8% agarose containing erlotinib in 6-well culture plates and incubated for 3 weeks. The plates were then stained with p-iodonitrotetrazolium violet (1 mg/ml) for 24 h at 37°C. The number of colonies of greater than 50 cells that formed was counted.

Flow cytometry analysis

For flow cytometry analysis, SUM149 cells were plated in 60-mm dishes, cultured overnight, and then treated with or without erlotinib. After 48 h, floating and adherent cells were collected by trypsinization, fixed overnight in 70% ethanol, and resuspended in propidium iodide (25 μg/mL) supplemented with 0.1% RNase A. DNA content was measured with a FACScan flow cytometer (BD Biosciences). These experiments were repeated 3 times independently.

Immunofluorescence and immunohistochemical analyses

Immunofluorescence analyses were performed as previously described (32). For immunofluorescence analysis, primary antibodies were anti-E-cadherin (Zymed Laboratories; catalog 33-4000), anti-β-catenin (Santa Cruz Biotechnology; catalog sc-7199), and anti-vimentin (Chemicon International; catalog AB-1620). FITC-conjugated antibodies (Biosource, Carlsbad, CA, USA) were used as secondary antibodies for vimentin staining and Texas Red-conjugated antibodies (Invitrogen) for E-cadherin and β-catenin staining. Cells were counterstained with 4',6-diamidino-2-phenylindole (DAPI) before being mounted under glass coverslips and analyzed by confocal microscopy (FV300, Olympus). For

immunohistochemical analysis, tumors were fixed in 10% phosphate-buffered formaldehyde for 24 h, embedded in paraffin, and stained as previously described (32).

3-dimensional (3D) culture

Matrigel (BD Biosciences) was stored at −80°C. Before use, Matrigel was thawed on ice overnight. For the bottom layer, 65 μl of Matrigel solution per well was added into a 4-well chamber slide (Lab-Tek II; Nalge Nunc International) and incubated at 37°C for 30 min to allow the Matrigel to solidify. Then, 5×10^4 cells were resuspended in 500 μl of culture medium with 2% Matrigel and erlotinib on ice and added to the solidified bottom layer.

Animal xenograft studies

All animal experiments were approved by the institutional review board of The University of Texas M. D. Anderson Cancer Center. Luciferase-expressing SUM149 (SUM149-luc) cells were established by stably transfecting pEF1a-Luc-IRES-Neo vector (33) into SUM149 cells. These cells have a phenotype and proliferation rate similar to those of parental SUM149 cells. A total volume of 0.15 mL of SUM149-luc cell suspension containing 5×10^6 cells with 50% Matrigel was injected into the bottom left mammary fat pad of 6-week-old nu/nu mice. On day 22, mice with well-established tumors (tumor volume close to 100 mm^3) were randomly allocated to 4 groups and were treated with 0 (vehicle, control), 25, 50, or 100 mg/kg of erlotinib daily by oral gavage for 28 days. The control-group mice received 0.5% methyl cellulose vehicle treatment. Each treatment group was represented by 7 mice. Tumor volume was determined weekly by externally measuring the tumors in 2 dimensions using a caliper. Volume (V) was determined by the following equation, where L is length and W is width of the tumor: $V = (L \times W^2) \times 0.5$. Tumor growth inhibition (%) was calculated as: 1- (the tumor volume change of treatment group/the tumor volume change of control group). Antitumor efficacy was determined by the percentage tumor growth inhibition. Percentage tumor growth inhibition at the endpoint of the study was compared between the control group and each treated group.

Ex vivo luciferase imaging of mice

Metastatic tumors in lung were detected by ex vivo luciferase imaging (IVIS imaging system 100; Xenogen Corporation, Alameda, CA). Prior to imaging, mice were injected intraperitoneally with 150 mg of D-luciferin (Caliper Life Sciences, Hopkinton, MA) per kg of body weight. Five minutes later, all animals were euthanized by cervical dislocation under isoflurane anesthesia, and lung tissues were collected immediately and then subjected to imaging for another 5 min. Fisher's exact test was used to determine whether there was any difference in the incidence of lung metastasis between control and erlotinib-treated groups.

Statistical analysis

Statistical analyses were performed using commercially available software (Statview, version 5.0, SAS Institute, Cary, NC). Two-sided unpaired Student's t-test was used for comparison between controls and treated groups. Statistical significance was defined as $P < 0.05$.

Results

Depletion of EGFR inhibits proliferation of IBC cells

We first tested the expression levels of EGFR and HER2 in 2 IBC cell lines, SUM149 and KPL-4. Western blot analysis showed that SUM149 cells have high expression of EGFR and low expression of HER2 and that KPL-4 cells have high expression of both EGFR and HER2 (Fig. 1A).

We then tested whether the EGFR pathway is intact in these 2 IBC cell lines by treating cells with EGF stimulation. Phosphorylation of EGFR was upregulated by EGF stimulation in both cell lines (Fig. 1B). Activation of Akt and extracellular signal-regulated kinases (ERK) 1/2, which are downstreams of the EGFR pathway in cell proliferation and survival mechanisms, was also detected after EGF stimulation (Fig. 1B), suggesting that the EGFR pathway is functional in IBC cells. We then examined the effect of siRNA-mediated EGFR inhibition on IBC cell proliferation. EGFR siRNA knockdown cells proliferated much more slowly than control siRNA-treated cells, suggesting that EGFR plays an important role in the proliferation of IBC cells (Fig. 1C and D).

Erlotinib inhibits proliferation and anchorage-independent growth of IBC cells, and this inhibitory activity of erlotinib is ERK dependent

Since EGFR siRNA knockdown inhibited IBC cell proliferation, we further studied the biological effect of EGFR tyrosine kinase inhibitor erlotinib on IBC cells. As expected, erlotinib significantly inhibited tyrosine phosphorylation of EGFR, Akt, and ERK in SUM149 and KPL-4 cells (Fig. 2A). We then tested the erlotinib sensitivity of both EGFR-overexpressing IBC cell lines, SUM149 and KPL-4, and EGFR-overexpressing non-IBC cell lines, MDA-MB-468 and BT-20 (30), by WST-1 cell proliferation assay and found that the median inhibitory concentration [IC_{50}] was 0.90 μM for SUM149 and 2.49 μM for KPL-4 cells, whereas it was more than 10 μM for MDA-MB-468 and BT-20 cells (Fig. 2B). Thus, the EGFR-overexpressing IBC cells were much more sensitive to erlotinib than were the non-IBC EGFR-overexpressing cells. Erlotinib induced G1 cell cycle arrest in SUM149 cells by FACScan analysis (Fig. 2C). To study the impact of erlotinib on anchorage-independent growth of IBC, SUM149 and KPL-4 cells were plated in soft agar and examined for differences in colony formation. We found that erlotinib-treated cells developed much fewer colonies in soft agar than untreated cells (Fig. 2D).

Because SUM149 cells have active EGFR pathways, we studied the role of ERK in SUM149. We induced ERK activation by transiently transfecting constitutively active MEK1 (CA-MEK1) (28) into SUM149 cells (Fig. 3A) and then treated them with erlotinib. We found that the cell viability of CA-MEK1-transfected cells after erlotinib treatment was markedly increased compared with that of empty vector-transfected cells, indicating that ERK activation made SUM149 cells more resistant to erlotinib (Fig. 3B). We then performed ERK siRNA knockdown in SUM149 cells and treated them with erlotinib (Fig. 3C). We found that ERK siRNA knockdown cells were more sensitive to erlotinib than control siRNA knockdown cells (Fig. 3D). Furthermore, inhibition of ERK activity by MEK inhibitors PD184161 and U0126 also sensitized SUM149 cells to erlotinib (data not shown). The role of ERK in another IBC cell line, KPL-4, was also studied. We performed ERK siRNA knockdown in KPL-4 cells and then treated them with erlotinib (Supplementary Fig. S1A). We found that ERK siRNA knockdown cells were more sensitive to erlotinib than were control siRNA knockdown cells (Supplementary Fig. S1B). Interestingly, even though pAkt is also significantly inhibited by erlotinib treatment (Fig. 2A), inhibition of Akt activity by the PI3K inhibitor LY29004 did not enhance the antiproliferative activity of erlotinib in SUM149 cells (Supplementary Fig. S2), suggesting that erlotinib inhibits IBC growth not through the Akt pathway. In summary, these data indicated that erlotinib inhibits IBC growth through the ERK pathway in both EGFR-positive SUM149 and EGFR-positive KPL-4 cells.

Erlotinib inhibits the motility and invasiveness of SUM149 cells and reverses the mesenchymal phenotype of IBC cells in 3D culture

Because patients with IBC are at high risk for recurrence in the form of metastatic disease, we first examined the motility of SUM149 cells by transwell migration assay after erlotinib treatment. As expected, cell migration was significantly inhibited by both a low dose (0.1 μM)

and a high dose of erlotinib (1 μM) (Fig. 4A). Similarly, erlotinib impaired the invasion of SUM149 cells in Matrigel invasion assay (Fig. 4B). Interestingly, the inhibition of migration and invasion seen following exposure of SUM149 cells to 0.1 μM erlotinib occurred in the absence of reduced cell viability. The activity of erlotinib in migration and invasion was also examined in EGFR-overexpressing non-IBC MDA-MB-468 cells. Compared with IBC cells, the cell motility and invasiveness were not inhibited by erlotinib in MDA-MB-468 cells (Fig. 4C and D).

After confirming the inhibition of motility and invasiveness by erlotinib and because EGFR overexpression was previously found to be more metastatic in IBC patients, we hypothesized that EGFR suppression inhibits metastasis of IBC. In 2-dimensional (2D) culture condition, both SUM149 and KPL-4 cells showed an epithelial phenotype characterized by localization of E-cadherin and β-catenin at sites of cell-cell contact (Fig. 5A and data not shown). When we cultured IBC cells in a 3D culture system, both SUM149 and KPL-4 cells exhibited a mesenchymal-like phenotype (Fig. 5B, left panel). These mesenchymal-looking cells exhibited reduced expression of the epithelial marker E-cadherin and significantly increased expression of the mesenchymal marker vimentin compared with the cells in 2D culture (Fig. 5C, top panels). However, when these cells in 3D culture were treated with erlotinib, the mesenchymal-like phenotype changed to an epithelial-cell phenotype (Fig. 5B, middle and right panels). Interestingly, the concentration of erlotinib that reversed the mesenchymal phenotype (0.1 μM) was 1 log lower than the concentration that inhibited proliferation (1 μM). Erlotinib induced upregulation of E-cadherin and downregulation of vimentin and recovered β-catenin in the cell membrane in 3D culture, which is consistent with the epithelial phenotype (Fig. 5C, middle and lower panels). These data indicated that erlotinib can inhibit EMT of EGFR-expressing IBC cells and suggested that erlotinib might have antimetastatic activity against IBC.

Because the antiproliferative activity of erlotinib is ERK dependent, we depleted ERK by ERK siRNA knockdown in SUM149 cells and then plated the cells in 3D culture. We found that ERK siRNA knockdown reversed the mesenchymal phenotype of SUM149 cells in 3D culture (Fig. 5*D*), suggesting that ERK plays an important role in EMT of IBC.

Erlotinib inhibits tumor growth and metastasis in a SUM149 xenograft model

After observing that erlotinib reduced cell proliferation and reversed the mesenchymal phenotype of SUM149 IBC cells *in vitro*, we hypothesized that erlotinib inhibits tumor growth and metastasis in a SUM149 breast cancer xenograft model. To address this hypothesis, we generated a SUM149 xenograft model by implanting SUM149-luc cells into the mammary fat pads of athymic nude mice. SUM149 tumors were readily apparent in mammary fat pads after 14 days and grew rapidly. Beginning 3 weeks after tumor cell implantation, the mice were treated with erlotinib administered by oral gavage daily for another 4 weeks. To identify the optimal doses that inhibit tumor growth and/or metastasis, we treated mice with SUM149 xenografts with 3 different doses of erlotinib: 25, 50, and 100 mg per kilogram of body weight. Treatment with 50 or 100 mg/kg/day erlotinib was chosen based on previous antitumor activity of erlotinib (34,35).

The higher doses (50 and 100 mg/kg) of erlotinib showed significant tumor-growth inhibition in the SUM149 xenograft model. On day 49, mean tumor-growth inhibition was 84% in the 50 mg/kg group ($P < 0.0001$) and 103% in the 100 mg/kg group ($P < 0.0001$) compared with the control group. Some tumor growth inhibition (43%) was observed in the 25 mg/kg group, but this inhibition was not significant compared to the control group ($P = 0.06$) (Fig. 6A).

To evaluate the antimetastatic activity of erlotinib in IBC, at the endpoint of animal study, we collected lung tissues from mice and then performed ex vivo luciferase imaging to detect spontaneous lung metastases in the mice with SUM149 xenograft tumors (Fig. 6B). The

metastatic tumors in bioluminescence-positive lung tissues were further confirmed by hematoxylin and eosin staining (Fig. 6B). Bioluminescence-positive lungs, indicating the presence of metastatic tumors, were detected in 3 of 7 mice (43%) in the control group. However, no bioluminescence-positive lungs were detected in mice in the 3 erlotinib-treated groups, indicating that erlotinib inhibited metastasis of IBC ($P = 0.04$) (Fig. 6C). Finally, we examined the expression of phosphorylated EGFR, phosphorylated ERK, and EMT markers in the primary tumor tissues by immunohistochemistry. As expected, the expression of phosphorylated EGFR and phosphorylated ERK was significantly inhibited in erlotinib-treated tumors compared to control tumors (Fig. 6D). More importantly, erlotinib increased the expression of E-cadherin and lowered the expression of vimentin in all erlotonib-treated tumors compared with control tumors (Fig. 6D). In conclusion, inhibition of lung metastasis and reversal from mesenchymal to epithelial phenotype was observed even in the low-dose condition (25 mg/kg erlotinib) that had no significant impact on primary tumor growth.

Discussion

In this report, we provide evidence that EGFR is a relevant target in IBC. Our novel finding here is that EGFR TKI erlotinib inhibited cell motility and invasiveness and reversed a mesenchymal phenotype of IBC cells to an epithelial phenotype at a low concentration that did not induce cytotoxicity (Fig. 4 and 5). This finding was further confirmed by our finding of *in vivo* antimetastatic activity despite limited antitumor activity at a low dose of erlotinib (Fig. 6). Erlotinib-treated tumors showed high expression of the epithelial marker E-cadherin and low expression of the mesenchymal marker vimentin compared with vehicle-treated tumors, suggesting that the antimetastatic activity of erlotinib may be through EMT inhibition. As expected, we found that the EGFR TKI erlotinib at a higher concentration showed dramatic antiproliferative activity against IBC both *in vitro* and *in vivo*, and this antiproliferative activity was ERK dependent.

One of our most interesting findings was that erlotinib reversed the mesenchymal phenotype to an epithelial phenotype in IBC cells in 3D culture. As shown in Fig. 4 and Fig. 5B and C, we found that a low concentration of erlotinib (0.1 μM) inhibited cell motility and invasion and reversed the mesenchymal phenotype to an epithelial phenotype, even though this concentration did not inhibit cell proliferation. More importantly, a low dose of erlotinib (25 mg/kg) inhibited lung metastasis in our xenograft model despite continuing growth of the primary tumors (Fig. 6). Those erlotinib-treated tumors had increased expression of E-cadherin and reduced expression of vimentin. Therefore, both our *in vitro* and our *in vivo* findings suggest that a low dose of erlotinib might be able to inhibit EMT and therefore metastasis of IBC even if this dose does not shrink the primary tumor. Typically, efficacy in phase II cancer clinical trials is measured in terms of the effect of treatment on tumor size (tumor response) but not metastasis. Our findings reported here suggest that for drugs like erlotinib, not only tumor shrinkage but also time-dependent endpoints of no recurrence, which may reflect metastasis inhibition, might be used as indicators of clinical drug efficacy. Our study may prompt the development of a therapeutic approach for preventing IBC metastasis by continuously delivering low doses of EGFR TKIs such as erlotinib to IBC patients in the adjuvant setting.

The mitogen-activated protein kinase (MAPK)-ERK pathway is known to promote cell proliferation, differentiation, survival, and metastasis (36,37). It has been reported that blockade of the MAPK pathway suppresses growth of colon tumors and melanoma metastasis *in vivo* (38,39), supporting the therapeutic value of blocking ERK signaling in cancer. Here, we have provided evidence that erlotinib's antiproliferative activity and conversion of mesenchymal to epithelial phenotype in IBC is ERK dependent, with ERK siRNA knockdown

cells showing greater sensitivity to erlotinib. Our data suggest that combining erlotinib therapy with inhibition of the ERK pathway may improve the therapeutic outcome in IBC.

In a phase II trial of the dual HER2/EGFR TKI lapatinib in IBC patients (25), lapatinib showed clinical activity against HER2-overexpressing IBC but produced no clinical responses in EGFR-expressing, HER2-negative IBC. In agreement with those findings, we recently found, in a study in which we used siRNA to knock down either EGFR or HER2 in EGFR-expressing, HER2-overexpressing non-inflammatory breast cancer cells, that lapatinib activity was dependent on HER2 activity but not EGFR activity in these cells (29). In the present study, an EGFR TKI, erlotinib, showed activity not only against EGFR-expressing, HER2-overexpressing KPL-4 IBC cells but also against EGFR-expressing, HER2-negative SUM149 IBC cells. Taken together, these findings warrant further investigation of erlotinib monotherapy in EGFR-expressing IBC, regardless of HER2 status, or combination therapy with lapatinib and the HER2-targeted monoclonal antibody trastuzumab in EGFR/HER2-expressing IBC.

In conclusion, we have demonstrated that EGFR can reverse a mesenchymal phenotype of IBC cells to epithelial phenotype and that the EGFR TKI erlotinib can reduce metastasis of IBC, possibly through inhibition of EMT. Thus, EGFR is an important target in IBC. Our novel insights might lead to development of novel therapeutic approaches for EGFR-expressing IBC, such as targeting EGFR and the ERK pathway simultaneously to inhibit tumor growth and metastasis.

Statement of Translational Relevance

To date, survival statistics have been grim for patients diagnosed with inflammatory breast cancer (IBC), the most aggressive form of breast cancer. It is therefore critical that we develop novel therapeutic strategies to treat IBC, which can rapidly metastasize. In this study, we defined the role of epidermal growth factor receptor (EGFR) in IBC by testing the antitumor and antimetastatic activity of an EGFR tyrosine kinase inhibitor, erlotinib. We determined that EGFR-targeted therapy is an effective treatment for IBC. Our preclinical findings lay an important foundation for the development of clinical trials of targeting of EGFR to inhibit IBC tumor growth and metastasis. We expect that this study will lead to new treatments that improve the quality of life of IBC patients by reducing disease recurrence and preventing its metastasis.

Supplementary Material

Refer to Web version on PubMed Central for supplementary material.

Acknowledgments

Grant support: This work was supported by NIH grant R01 CA123318-01A1, Morgan Welch Inflammatory Breast Cancer Research Program, State of Texas Rare and Aggressive Breast Cancer Research Program Grant (NT. Ueno), and Susan G. Komen Postdoctoral Fellowship Grant KG091192 (D. Zhang).

We thank Dr. Junichi Kurebayashi (Kawasaki Medical School, Japan) for providing KPL-4 cells; Ms. Linda X. H. Yuan (Department of Breast Medical Oncology, The University of Texas M. D. Anderson Cancer Center) for technical assistance; and Ms. Stephanie P. Deming (Department of Scientific Publications, The University of Texas M. D. Anderson Cancer Center) for editorial assistance.

References

1. Cristofanilli M, Buzdar AU, Hortobagyi GN. Update on the management of inflammatory breast cancer. Oncologist 2003;8:141–148. [PubMed: 12697939]

2. Kleer CG, van Golen KL, Merajver SD. Molecular biology of breast cancer metastasis. Inflammatory breast cancer: clinical syndrome and molecular determinants. Breast Cancer Res 2000;2:423–429. [PubMed: 11250736]
3. Anderson WF, Schairer C, Chen BE, Hance KW, Levine PH. Epidemiology of inflammatory breast cancer (IBC). Breast Dis 2005;22:9–23. [PubMed: 16735783]
4. Jaiyesimi IA, Buzdar AU, Hortobagyi G. Inflammatory breast cancer: a review. J Clin Oncol 1992;10:1014–1024. [PubMed: 1588366]
5. Chang S, Parker SL, Pham T, Buzdar AU, Hursting SD. Inflammatory breast carcinoma incidence and survival: the surveillance, epidemiology, and end results program of the National Cancer Institute, 1975–1992. Cancer 1998;82:2366–2372. [PubMed: 9635529]
6. Levine PH, Steinhorn SC, Ries LG, Aron JL. Inflammatory breast cancer: the experience of the surveillance, epidemiology, and end results (SEER) program. J Natl Cancer Inst 1985;74:291–297. [PubMed: 3856043]
7. Edme N, Downward J, Thiery JP, Boyer B. Ras induces NBT-II epithelial cell scattering through the coordinate activities of Rac and MAPK pathways. Journal of cell science 2002;115:2591–2601. [PubMed: 12045229]
8. Jechlinger M, Grunert S, Tamir IH, et al. Expression profiling of epithelial plasticity in tumor progression. Oncogene 2003;22:7155–7169. [PubMed: 14562044]
9. Thiery JP. Epithelial-mesenchymal transitions in development and pathologies. Current opinion in cell biology 2003;15:740–746. [PubMed: 14644200]
10. Sarrio D, Rodriguez-Pinilla SM, Hardisson D, Cano A, Moreno-Bueno G, Palacios J. Epithelial-mesenchymal transition in breast cancer relates to the basal-like phenotype. Cancer Res 2008;68:989–997. [PubMed: 18281472]
11. Slamon DJ, Clark GM, Wong SG, Levin WJ, Ullrich A, McGuire WL. Human breast cancer: correlation of relapse and survival with amplification of the HER-2/neu oncogene. Science 1987;235:177–182. [PubMed: 3798106]
12. Slamon DJ, Godolphin W, Jones LA, et al. Studies of the HER-2/neu proto-oncogene in human breast and ovarian cancer. Science 1989;244:707–712. [PubMed: 2470152]
13. Olayioye MA, Neve RM, Lane HA, Hynes NE. The ErbB signaling network: receptor heterodimerization in development and cancer. Embo J 2000;19:3159–3167. [PubMed: 10880430]
14. Cerra M, Cecco L, Montella M, Tuccillo F, Bonelli P, Botti G. Epidermal growth factor receptor in human breast cancer comparison with steroid receptors and other prognostic factors. Int J Biol Markers 1995;10:136–142. [PubMed: 8551055]
15. Seshadri R, McLeay WR, Horsfall DJ, McCaul K. Prospective study of the prognostic significance of epidermal growth factor receptor in primary breast cancer. Int J Cancer 1996;69:23–27. [PubMed: 8600054]
16. Berger MS, Gullick WJ, Greenfield C, Evans S, Addis BJ, Waterfield MD. Epidermal growth factor receptors in lung tumours. The Journal of pathology 1987;152:297–307. [PubMed: 3668732]
17. Yarden Y, Sliwkowski MX. Untangling the ErbB signalling network. Nature reviews 2001;2:127–137.
18. Cox G, Jones JL, O'Byrne KJ. Matrix metalloproteinase 9 and the epidermal growth factor signal pathway in operable non-small cell lung cancer. Clin Cancer Res 2000;6:2349–2355. [PubMed: 10873086]
19. Ohsaki Y, Tanno S, Fujita Y, et al. Epidermal growth factor receptor expression correlates with poor prognosis in non-small cell lung cancer patients with p53 overexpression. Oncology reports 2000;7:603–607. [PubMed: 10767376]
20. Volm M, Rittgen W, Drings P. Prognostic value of ERBB-1, VEGF, cyclin A, FOS, JUN and MYC in patients with squamous cell lung carcinomas. British journal of cancer 1998;77:663–669. [PubMed: 9484827]
21. Moore MJ, Goldstein D, Hamm J, et al. Erlotinib plus gemcitabine compared with gemcitabine alone in patients with advanced pancreatic cancer: a phase III trial of the National Cancer Institute of Canada Clinical Trials Group. J Clin Oncol 2007;25:1960–1966. [PubMed: 17452677]
22. Shepherd FA, Rodrigues Pereira J, Ciuleanu T, et al. Erlotinib in previously treated non-small-cell lung cancer. N Engl J Med 2005;353:123–132. [PubMed: 16014882]

23. Baselga J, Albanell J, Ruiz A, et al. Phase II and tumor pharmacodynamic study of gefitinib in patients with advanced breast cancer. J Clin Oncol 2005;23:5323–5333. [PubMed: 15939921]
24. Tan AR, Yang X, Hewitt SM, et al. Evaluation of biologic end points and pharmacokinetics in patients with metastatic breast cancer after treatment with erlotinib, an epidermal growth factor receptor tyrosine kinase inhibitor. J Clin Oncol 2004;22:3080–3090. [PubMed: 15284258]
25. Johnston S, Trudeau M, Kaufman B, et al. Phase II study of predictive biomarker profiles for response targeting human epidermal growth factor receptor 2 (HER-2) in advanced inflammatory breast cancer with lapatinib monotherapy. J Clin Oncol 2008;26:1066–1072. [PubMed: 18212337]
26. Cabioglu N, Gong Y, Islam R, et al. Expression of growth factor and chemokine receptors: new insights in the biology of inflammatory breast cancer. Ann Oncol 2007;18:1021–1029. [PubMed: 17351259]
27. Kurebayashi J, Otsuki T, Tang CK, et al. Isolation and characterization of a new human breast cancer cell line, KPL-4, expressing the Erb B family receptors and interleukin-6. British journal of cancer 1999;79:707–717. [PubMed: 10070858]
28. Yang JY, Zong CS, Xia W, et al. ERK promotes tumorigenesis by inhibiting FOXO3a via MDM2-mediated degradation. Nat Cell Biol 2008;10:138–148. [PubMed: 18204439]
29. Zhang D, Pal A, Bornmann WG, et al. Activity of lapatinib is independent of EGFR expression level in HER2-overexpressing breast cancer cells. Mol Cancer Ther 2008;7:1846–1850. [PubMed: 18644997]
30. Yamasaki F, Zhang D, Bartholomeusz C, et al. Sensitivity of breast cancer cells to erlotinib depends on cyclin-dependent kinase 2 activity. Mol Cancer Ther 2007;6:2168–2177. [PubMed: 17671085]
31. Ueno NT, Yu D, Hung MC. Chemosensitization of HER-2/neu-overexpressing human breast cancer cells to paclitaxel (Taxol) by adenovirus type 5 E1A. Oncogene 1997;15:953–960. [PubMed: 9285690]
32. Zhang D, Hirota T, Marumoto T, et al. Cre-loxP-controlled periodic Aurora-A overexpression induces mitotic abnormalities and hyperplasia in mammary glands of mouse models. Oncogene 2004;23:8720–8730. [PubMed: 15480417]
33. Singh B, Berry JA, Shoher A, Ayers GD, Wei C, Lucci A. COX-2 involvement in breast cancer metastasis to bone. Oncogene 2007;26:3789–3796. [PubMed: 17213821]
34. Friess T, Scheuer W, Hasmann M. Combination treatment with erlotinib and pertuzumab against human tumor xenografts is superior to monotherapy. Clin Cancer Res 2005;11:5300–5309. [PubMed: 16033849]
35. Ouchi KF, Yanagisawa M, Sekiguchi F, Tanaka Y. Antitumor activity of erlotinib in combination with capecitabine in human tumor xenograft models. Cancer chemotherapy and pharmacology 2006;57:693–702. [PubMed: 16362295]
36. Roberts PJ, Der CJ. Targeting the Raf-MEK-ERK mitogen-activated protein kinase cascade for the treatment of cancer. Oncogene 2007;26:3291–3310. [PubMed: 17496923]
37. Treisman R. Regulation of transcription by MAP kinase cascades. Current opinion in cell biology 1996;8:205–215. [PubMed: 8791420]
38. Sebolt-Leopold JS, Dudley DT, Herrera R, et al. Blockade of the MAP kinase pathway suppresses growth of colon tumors in vivo. Nat Med 1999;5:810–816. [PubMed: 10395327]
39. Collisson EA, De A, Suzuki H, Gambhir SS, Kolodney MS. Treatment of metastatic melanoma with an orally available inhibitor of the Ras-Raf-MAPK cascade. Cancer Res 2003;63:5669–5673. [PubMed: 14522881]

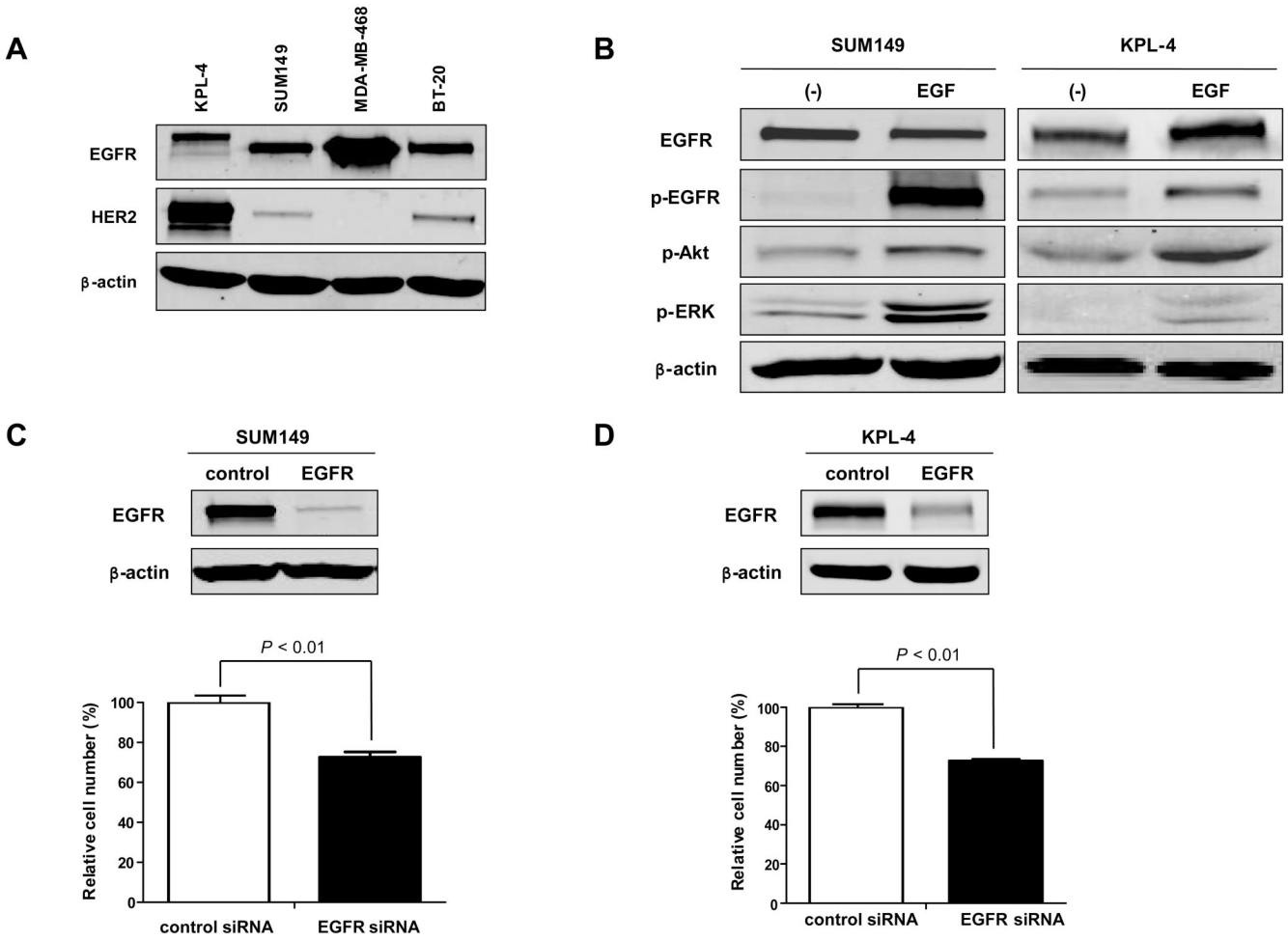

Fig. 1.

EGFR promotes IBC cell proliferation. *A*, Western blot analysis was performed to detect the expression levels of EGFR and HER2 in 2 IBC cell lines, KPL-4 and SUM149, and 2 non-IBC cell lines, MDA-MB-468 and BT-20. β-actin was used as a loading control. *B*, SUM149 and KPL-4 cells were cultured in serum-free medium for 24 h and then exposed to EGF in culture medium at a concentration of 100 ng/ml for 5 min. Western blot analysis was performed to detect EGFR and phosphorylated (p-) EGFR, p-Akt, and p-ERK. β-actin was used as a loading control. *C* and *D*, SUM149 (C) and KPL-4 (*D*) cells were treated with control siRNA or EGFR siRNA for 72 h, and cell viability was measured by WST-1 assay. Western blot analysis was performed to determine the expression level of EGFR after siRNA knockdown. Viability of EGFR siRNA knockdown cells was compared with that of control siRNA knockdown cells. *P* values are indicated. Each experiment was repeated 3 times independently.

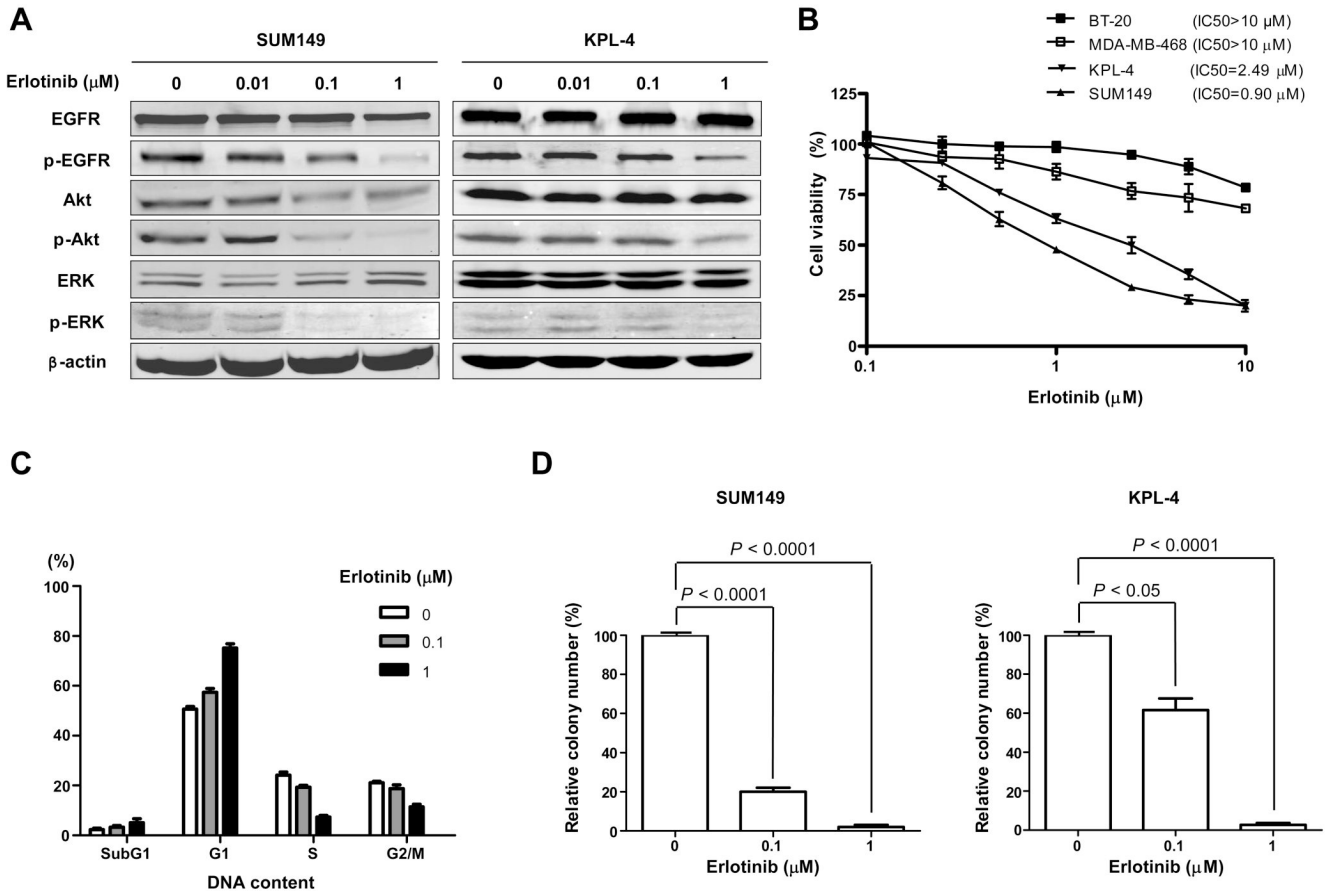

Fig. 2.

IBC cells are sensitive to erlotinib. *A*, SUM149 and KPL-4 cells were treated with 0 (vehicle), 0.01, 0.1, or 1 μM erlotinib for 72 h. Western blot analysis was performed to detect EGFR, p-EGFR, Akt, p-Akt, ERK, and p-ERK. β-actin was used as a loading control. *B*, SUM149, KPL-4, MDA-MB-468, and BT-20 cells were plated in 96-well plates and treated with 0.1, 0.25, 0.5, 1, 2.5, 5, or 10 μM erlotinib for 3 days. WST-1 assay was performed to quantify the activity of erlotinib. *C*, SUM149 cells were treated with 0, 0.1, or 1 μM erlotinib for 48 h, and FACScan analysis was performed to detect the cell cycle distribution. *D*, SUM149 and KPL-4 cells were plated in soft agar with 0, 0.1, or 1 μM erlotinib to determine the anchorage-independent growth. Differences in the colony numbers were measured 21 days later. *P* values are indicated. Each experiment was repeated 3 times independently.

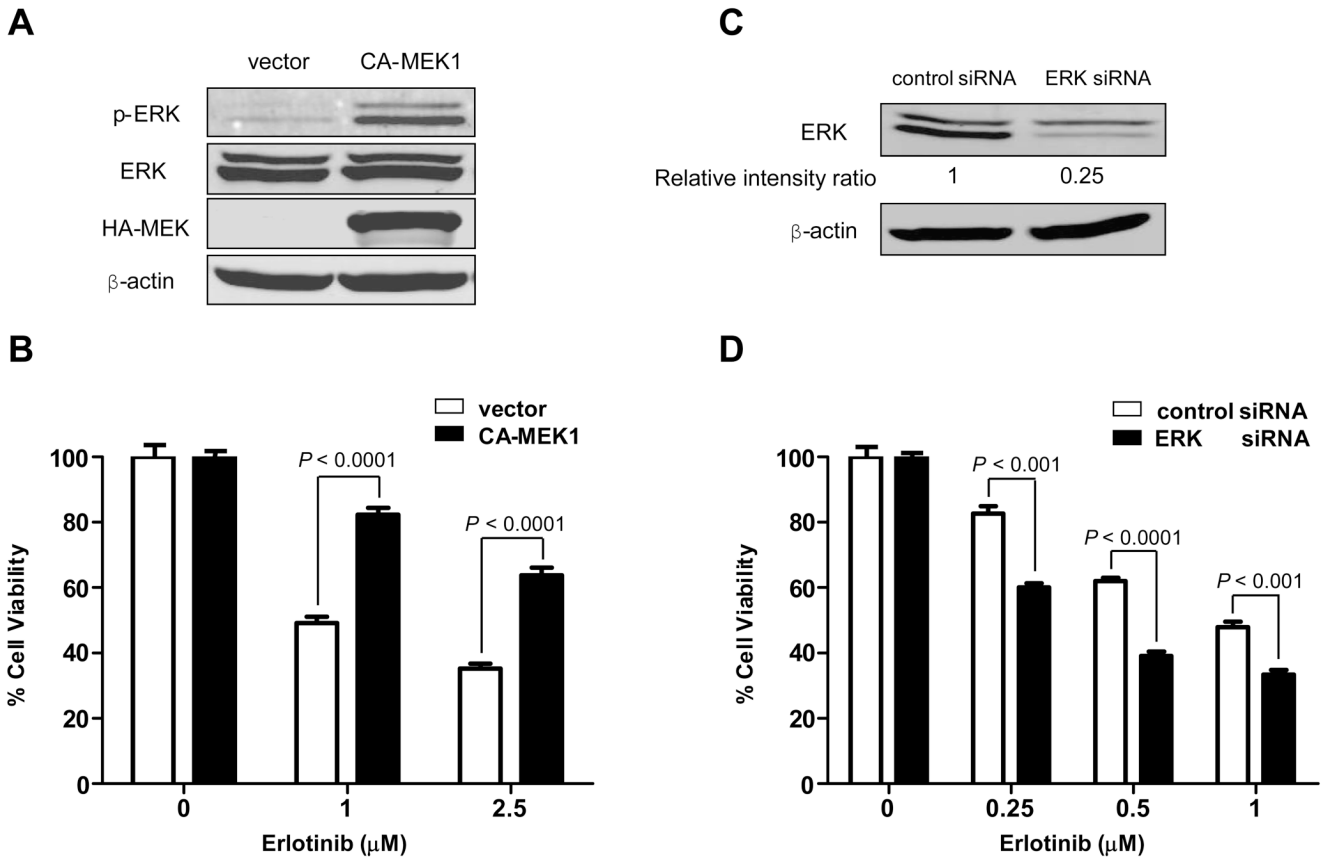

Fig. 3.

Erlotinib inhibits SUM149 cell proliferation through the ERK pathway. *A*, SUM149 cells were transfected with empty vector or CA-MEK1 for 72 h. Western blot analysis was performed to determine the level of activated ERK after CA-MEK1 transfection. *B*, Beginning 72 h after CA-MEK1 transfection, SUM149 cells were treated with the indicated concentrations of erlotinib for another 72 h, and then the proliferation-inhibitory effect of erlotinib was quantified by WST-1 assay. *C*, SUM149 cells were treated with control siRNA or ERK siRNA for 72 h. Western blot analysis was performed to determine the expression level of ERK after siRNA knockdown. The density values for the bands were measured by using the NIH Image program. The intensity ratio of ERK protein to its internal control band (β-actin) was relative to the ratio from the negative control siRNA, which was normalized as 1. *D*, Beginning 72 h after siRNA knockdown, SUM149 cells were treated with the indicated concentrations of erlotinib for another 72 h. Proliferation-inhibitory effects of erlotinib were quantified by WST-1 assay. Viability of ERK-siRNA-knockdown cells was compared with that of control-siRNA-treated cells. *P* values are indicated. Each experiment was repeated 3 times independently.

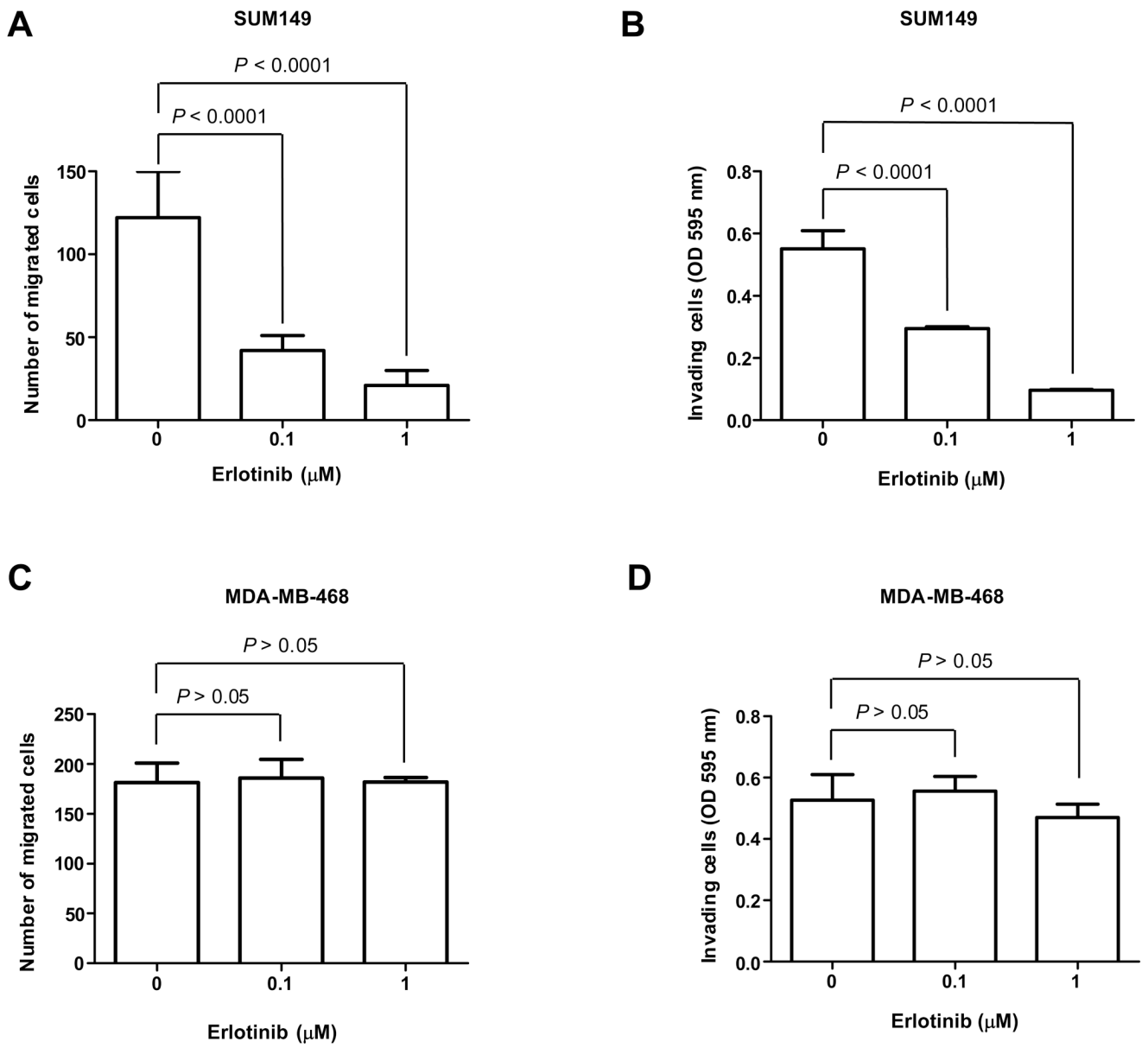

Fig. 4.

Erlotinib inhibits SUM149 cell motility and invasion. *A*, SUM149 cells were evaluated for their motility by transwell migration assay following 48 h treatment with 0, 0.1, or 1 μM erlotinib and 6 h migration. Numbers of transwell-migrated cells were counted. *B*, SUM149 cells were treated with 0, 0.1, or 1 μM erlotinib for 48 h and then subjected to an invasion assay for another 24 h and assayed for their ability to invade through Matrigel. OD595 nm values correspond to the low side of the filter and represent the mean of 3 determinations. *C*, Transwell migration assay described in (*A*) was performed in MDA-MB-468 cells. *D*, Matrigel invasion assay described in (*B*) was performed in MDA-MB-468 cells. *P* values are indicated.

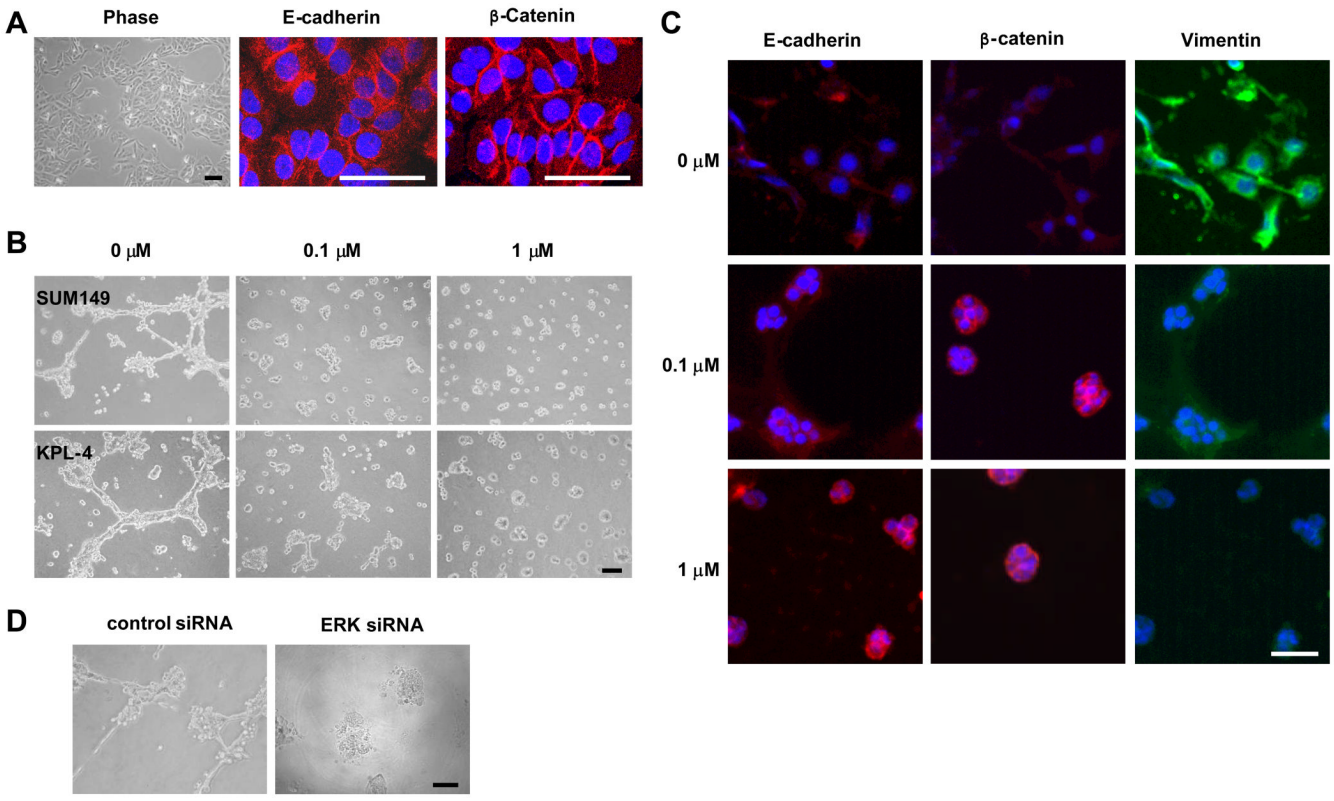

Fig. 5.

Erlotinib reverses the mesenchymal phenotype of SUM149 cells in 3D culture. *A*, Phase-contrast picture (Phase) of SUM149 cells in 2D culture. Immunofluorescence analysis was performed by using anti-E-cadherin and anti-β-catenin antibodies in SUM149 cells. Nuclei were visualized with DAPI. *B*, SUM149 (top panels) and KPL-4 (bottom panels) cells were plated in 3D culture without or with erlotinib (0.1 or 1 μM) and cultured for 48 h. The phenotypes were shown by using a phase contrast microscope. *C*, SUM149 cells were plated in 3D culture without or with erlotinib for 4 days. Immunofluorescence analysis was performed to detect E-cadherin, β-catenin, and vimentin. Nuclei were visualized with DAPI. *D*, SUM149 cells were transfected with control or ERK siRNA for 48 h and then plated in 3D culture for another 48 h. The phenotypes were shown by using a phase contrast microscope. Bars, 50 μm.

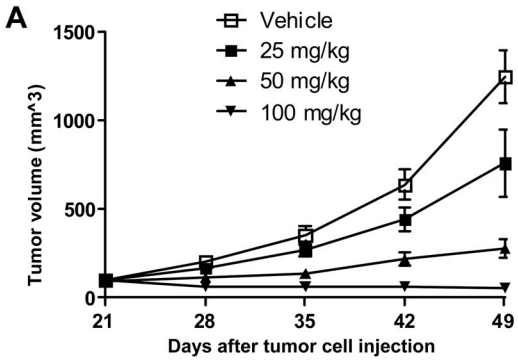

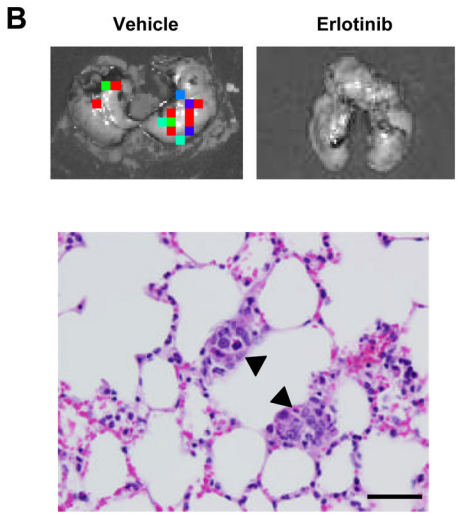

C

Group	No. of Mice	Incidence of lung metastasis
control (vehicle)	3 of 7	(43%)
25 mg/kg erlotinib	0 of 7	(0%)
50 mg/kg erlotinib	0 of 7	(0%)
100 mg/kg erlotinib	0 of 7	(0%)

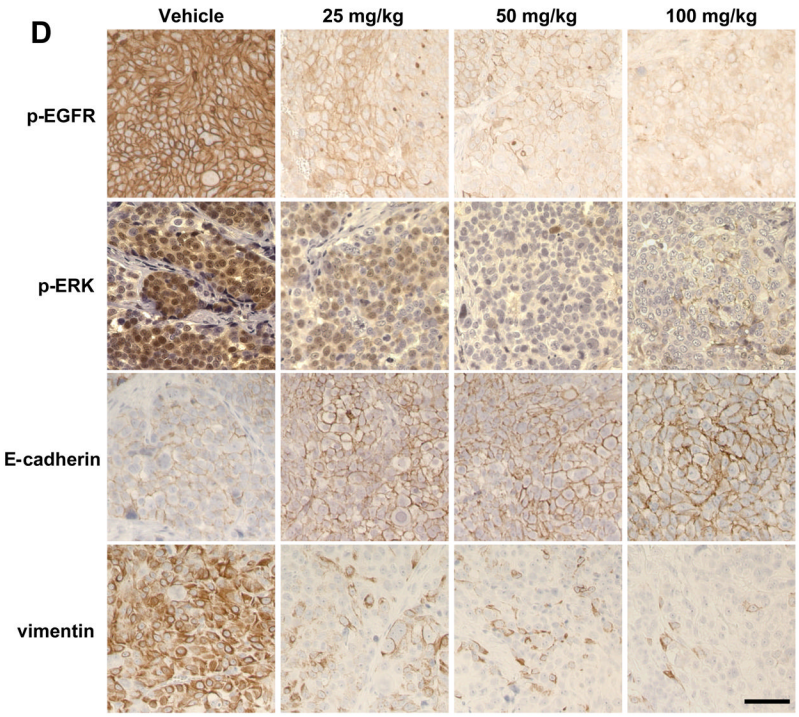

Fig. 6.

Erlotinib inhibits tumor growth and metastasis in a SUM149 xenograft model. *A*, Tumor volumes in 4 groups of mice (vehicle, 25, 50, and 100 mg/kg erlotinib) were measured weekly and calculated as described in Materials and Methods. Each data point represents the mean tumor volume of 7 mice per group; bars, SD. *B*, Findings on ex vivo imaging of lung tissues from a control (vehicle) mouse and a 25 mg/kg erlotinib-treated mouse to detect metastatic tumors (upper panels). Hematoxylin and eosin staining of a lung tissue section from a control mouse at the endpoint of the study showed 2 small deposits of metastatic tumors (arrowheads) in the alveolar septae (lower panel). *C*, Numbers of mice with metastatic tumor and the incidence of lung metastasis in 4 groups. *D*, Immunohistochemical analysis of p-EGFR, p-ERK, E-cadherin, and vimentin in tumor tissues of SUM149 xenografts. Bars, 50 μm.